

## Control of low-dimensional spatiotemporal chaos in Fourier space

Carlos Lourenço,<sup>1</sup> Marc Hougardy,<sup>2</sup> and Agnessa Babloyantz<sup>1</sup>

<sup>1</sup>*Service de Chimie-Physique, Université Libre de Bruxelles, Case Postale 231-Campus Plaine, 1050 Bruxelles, Belgium*

<sup>2</sup>*International Solvay Institute for Physics and Chemistry, 50, Avenue F.D. Roosevelt, 1050 Bruxelles, Belgium*

(Received 27 October 1994)

A method is proposed whereby spatiotemporal chaos with few degrees of freedom is controlled via small and occasional feedback perturbations. The state of the system is monitored in Fourier space, using the fact that a few major modes may account for the essentials of the dynamics. Several unstable periodic orbits showing spatiotemporal structure are stabilized in the one-dimensional Kuramoto-Sivashinsky equation in the chaotic regime. This equation constitutes a link between dissipative systems displaying low-dimensional temporal chaos and the phase turbulence seen in a class of extended systems described by partial differential equations.

PACS number(s): 05.45.+b, 47.52.+j, 82.20.Wt

The existence of spatiotemporal chaotic dynamics is well established for a variety of physical as well as physiologic systems [1,2]. In the recent literature on chaos, one finds several reports on the control of chaotic systems. The most popular method is the one proposed by Ott, Grebogi, and Yorke (OGY) [3], wherein very weak occasional perturbations are applied to the system and turn its erratic behavior into a periodic regime. This feedback control uses the fact that the chaotic attractor has embedded in it an infinite number of unstable periodic orbits (UPO's) [4,5], some of which may be selected for stabilization. Theoretical as well as experimental applications of this stabilization procedure are numerous [6–9]. Most of the work cited above concerns systems that can, in principle, be described by single maps or by a few coupled ordinary differential equations. Chaotic spatially extended systems have also been simulated and controlled as coupled map lattices [10], a moderate size network of Ginzburg-Landau oscillators [11], and model cortical networks [12]. All these cases show distributed control where units are individually acted upon. These concepts were used in a two interconnected layer of oscillatory units mimicking brain dynamics [13]. It was shown that stabilization of UPO's may induce "attentive" states that enable the model cortex to categorize patterns and motion without previous learning.

In this paper, we address the problem of controlling a class of space- and time-continuous systems described by partial differential equations. The spatiotemporal chaos considered arises from an instability in a small number of spatial modes in an oscillatory medium. The system evolves in a weakly nonlinear range and presents a phase turbulence regime with no amplitude defects. We propose a global control of the phase in this regime as opposed to a local control of the amplitude in defect turbulence [14]. Our approach consists of an extension of the OGY method after an expansion in an appropriate basis of space functions  $\{\phi_i\}$ . We consider a scalar function  $\psi(\vec{x}, t)$  that completely determines the state of a system described by  $A_\mu\psi = 0$  together with boundary conditions. Here  $\vec{x}$  and  $t$  are space and time variables, respectively, and  $A_\mu$  is a nonlinear operator containing space and time derivatives and depending on param-

eters  $\mu$ . We expand  $\psi = \sum_i a_i(t) \phi_i(\vec{x})$  and define a Euclidean phase space spanned by the  $a_i$ , where the dynamics will be followed. Control of chaos will be performed in the Fourier space thus defined. We further assume that although the system is infinite dimensional, the corresponding strange attractor can be spanned by few degrees of freedom. The asymptotic dynamics is characterized by a low-dimensional map  $F_\mu: \Pi \rightarrow \Pi$  in a hyperplane  $\Pi$  of the projection phase space spanned by the subset  $\{a_i\}_{i=1}^N$ ,  $N$  being finite. This defines a Poincaré section in Fourier space. UPO's of the original infinite-dimensional system are identified as fixed points or discrete-time periodic orbits of the map  $F_\mu$  on this Poincaré section. We illustrate the stabilization method in the case where  $F_\mu$  is one dimensional and  $\mu$  is a scalar. Thus the continuous time periodicity of the system can be related to the discrete time periodicity of a single observable.

We consider the first-return map  $a_2(n+1) = F_\mu[a_2(n)]$ , based on the Poincaré section defined by  $a_1 = a_1^*$ ,  $\dot{a}_1 < 0$ . If unperturbed, the system dynamics is governed by  $F_\mu$ . A fixed point  $a_2^*$  of this map corresponds to a period-one orbit of the original system, and its instability is a consequence of the condition  $|dF_\mu/da_2|_{a_2^*} > 1$ . Usually, the exponential dynamics near  $a_2^*$  is controlled by applying a small perturbation to the parameter  $\mu$  during one period of recurrence on the Poincaré section, and readjusting the value of the perturbation on every recurrence according to a simple feedback rule [3]. The procedure described in Ref. [3] is not applicable here because the parameter perturbation introduces a high-dimensional transient that typically lasts more than one recurrence period. Therefore, transient time is too long for control adjustments on every recurrence to succeed. An extension of the control method to high-dimensional systems was proposed in [15], where one considers the past history of parameter variations. Our algorithm relies only on the knowledge of the present state of the system at the moment of control. The prescription for control is as follows. If, at time  $n$ ,  $a_2$  is in a linear vicinity of  $a_2^*$ , apply a perturbation  $\delta\mu$  to  $\mu$  during  $\Delta t$ , say one period of recurrence on the Poincaré section. Then set  $\delta\mu = 0$  during  $m$  periods of recurrence. Although the perturbation  $\delta\mu$  temporarily drives the system away from the  $\mu$  attractor, if  $m$  is large enough

the second step allows the system to relax back into the original  $\mu$  attractor. The two-step procedure induces a temporary map  $a_2(n+m+1) = G^{(m+1)}[a_2(n), \delta\mu]$ . A method for estimating  $G$  will be suggested in the sequel.  $\delta\mu$  is chosen by solving  $a_2^* = G^{(m+1)}[a_2(n), \delta\mu]$ . Notice that  $G^{(m+1)}(a_2, 0) = F_\mu^{(m+1)}(a_2)$ . This action is performed every  $(m+1)$ th recurrence with different  $\delta\mu$  values so that the fixed point  $a_2^*$  is effectively stabilized regardless of the finite precision of the feedback. We take the smallest values of  $m$  for which the  $\mu$  attractor is repeatedly attained.  $m$  should not be made too large, because that would imply that the system could not be acted upon frequently enough to prevent it from escaping control. Taking, e.g.,  $m = 2$ , control actions can be performed every three recurrences. Because at the beginning of each control action the system is again in the  $\mu$  attractor, a repetitive control algorithm can be applied from there, regardless of the value of the previous control perturbations  $\delta\mu$ . Without the  $m$  recurrences relaxation time, the dependence of the control on previous parameter perturbations would prevent it from having the simple form seen above. We choose to stabilize fixed points of a  $(m+1)$ -return map  $F_\mu^{(m+1)}$ , where  $m$  is the same as above. These include fixed points of maps of order lower than  $(m+1)$ . For example, the fixed points of  $F_\mu^{(1)}$  and  $F_\mu^{(2)}$  appear also as fixed points of  $F_\mu^{(4)}$ . In other words, a fixed point of  $F_\mu^{(m+1)}$  is associated with an UPO of the continuous system that crosses the Poincaré section at most at  $(m+1)$  different locations per orbit, so that its actual period is at most  $(m+1)$ . We recall that the points mapped by  $F_\mu^{(m+1)}$  and  $G^{(m+1)}$  lie in a Fourier space and not in physical space.

The map  $G^{(m+1)}$  is estimated locally by perturbing during one recurrence an evenly distributed set of  $a_2$  points originally in the  $\mu$  attractor and close to  $a_2^*$ , then turning the perturbation off during  $m$  recurrences and watching where the next iterate will be at the end of these two combined actions. This is performed for a set of small  $\delta\mu$  values. The map  $G^{(m+1)}$  is then fitted via a least-squares algorithm.

The actual stabilization of UPO's is preceded by monitoring the successive values  $a_2(n)$ . As indicated above, the algorithm for control is applied when the linear vicinity of a chosen fixed point  $a_2^*$  is attained. This ensures that small  $\delta\mu$  suffice for control, and, therefore,  $G^{(m+1)}$  is linear in  $\delta\mu$ . No control action is performed if the necessary  $|\delta\mu|$  is greater than a maximum allowed  $|\delta\mu|_{\max}$ . The linearity condition renders the computation of the  $\delta\mu$  simple. Defining  $\delta a_2(n) = a_2(n) - a_2^*$ , we have, in the vicinity of  $a_2^*$ ,

$$\delta a_2(n+m+1) = \frac{\partial G^{(m+1)}}{\partial a_2} \delta a_2(n) + \frac{\partial G^{(m+1)}}{\partial \mu} \delta \mu, \quad (1)$$

with the derivatives evaluated at  $\delta\mu=0, \delta a_2=0$ . Notice that  $(\partial G^{(m+1)}/\partial a_2)_{\delta\mu=0, \delta a_2=0} = (dF_\mu^{(m+1)}/da_2)_{a_2^*}$ . The quantity relevant for the stabilization is the gain  $g = -(\partial G^{(m+1)}/\partial \mu)/((dF_\mu^{(m+1)}/da_2))$ , with the derivatives evaluated as indicated. Equating Eq. (1) to zero, we get the feedback law at iteration  $n$ ,  $\delta\mu = g^{-1}\delta a_2(n)$ . Al-

though the linearity assumption is not essential, it allows for an easier generalization to higher-dimensional control. As an effect of control,  $a_2(n)$  becomes  $(m+1)$  periodic. This results in all  $a_j(t)$  becoming time periodic, which, in turn, implies time periodicity of  $\psi(\vec{x}, t)$ .

We illustrate the stabilization method described above with the well-known Kuramoto-Sivashinsky equation (KSE) [1], which is an example of low-dimensional chaotic behavior with one spatial degree of freedom. The KSE appears in several physical contexts (see Refs. [16,17] and references therein), namely in the modeling of diffusion-induced phase turbulence [1], and it reads

$$\frac{\partial \tilde{u}}{\partial t} + \sigma \frac{\partial^2 \tilde{u}}{\partial x^2} + \frac{\partial^4 \tilde{u}}{\partial x^4} - \left( \frac{\partial \tilde{u}}{\partial x} \right)^2 = 0, \quad (2)$$

where  $-L/2 \leq x \leq L/2$  and  $\sigma$  is the diffusion coefficient. The real field  $\tilde{u}$  appearing in the KSE can be taken to represent the long-wavelength phaselike deviation from some reference structure. The related amplitudelike deviation can be viewed as constant, or at least adiabatically dependent on the longer time-scale phase deviation, so that it does not enter the evolution equation. The boundary conditions are  $\partial \tilde{u}/\partial x = \partial^3 \tilde{u}/\partial x^3 = 0$  for  $x = \pm L/2$ . It is easily seen that the space average  $\langle \tilde{u} \rangle(t)$  is increasing in time. In order to avoid this drift, we define a new function  $u(x, t) = \tilde{u}(x, t) - \langle \tilde{u} \rangle(t)$ . The function  $u$  is expanded in Fourier modes as [1]

$$u(x, t) = \sum_j \left[ A_j(t) \cos\left(\frac{2j\pi}{L}x\right) + B_j(t) \sin\left(\frac{(2j-1)\pi}{L}x\right) \right], \quad (3)$$

where  $A_j(t) = (2/L) \int_{-L/2}^{L/2} u(x, t) \cos\{[2j\pi/L]x\} dx$  and  $B_j(t) = (2/L) \int_{-L/2}^{L/2} u(x, t) \sin\{[(2j-1)\pi/L]x\} dx$  with  $j = 1, 2, \dots$ . Hence we project the general nonlinear dynamics in the basis of normal modes of the linearized space operator of Eq. (2). This is a natural choice in a weakly nonlinear range and amounts to a clear representation. A Euclidean space with a restricted number of  $A_j$  and  $B_j$  coordinates can then be defined. The uniform mode  $A_0$  is absent due to the drift correction. It can be shown that  $A_0$  does not influence the evolution of the remaining modes.

For  $L = 10.1$  and  $\sigma = 2.5$ , Eq. (2) exhibits spatiotemporal chaos. To characterize this chaos, we consider a Poincaré section in Fourier space, defined by  $A_1 = A_1^P = 3.16, \dot{A}_1 < 0$ . Measuring the values  $A_2(n)$  at successive crossings of the Poincaré hyperplane, we find that they are randomly distributed and that accordingly the return maps  $A_2(n+k) = F_\sigma^{(k)}[A_2(n)]$  are chaotic. Figure 1 shows the first-return map of  $A_2$ . Although this and higher order maps are not unimodal, not all branches are of interest for control. The system must stay on the same branch for a few iterations and exhibit exponential divergence from a fixed point, if uncontrolled. The transition between branches obeys to a well-defined sequence.

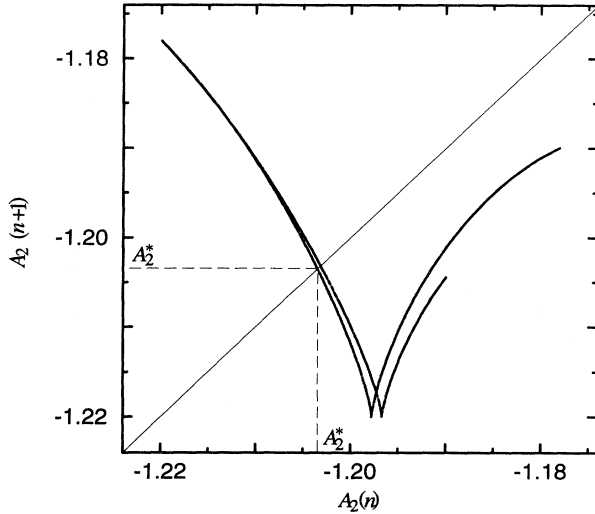


FIG. 1. Chaotic first-return map  $A_2(n+1)=F_\sigma[A_2(n)]$  on the Poincaré section  $A_1=A_1^P=3.16$ ,  $A_1<0$ . The  $A_j$  are the Fourier expansion coefficients of  $u$ , as defined in Eq. (3). Parameter values of the KSE are  $L = 10.1$  and  $\sigma = 2.5$ .  $F_\sigma$  is two valued for all  $A_2 < -1.19$ . The leftmost intersection of the bisectrix  $A_2(n+1) = A_2(n)$  with  $F_\sigma$  corresponds to the fixed point  $A_2^* = -1.2035$ .

For example, in Fig. 1 the exponential dynamics away from the fixed point  $A_2^*$  can be seen as successive points along the leftmost branch of  $F_\sigma$  and close to  $(A_2^*, A_2^*)$  (not shown). It is preceded by a single point in the rightmost branch of the map, with ordinate value close to  $A_2^*$ . Similar behavior is also observed with higher order maps.

Control of the chaotic regime is performed by way of the procedure outlined above.  $\sigma$  in Eq. (2) is the control parameter and is, therefore, allowed to have small departures  $\delta\sigma$  from its nominal value of 2.5. As explained above, maps of order higher than one are required by the method. We first plot  $F_\sigma^{(3)}$  and  $F_\sigma^{(4)}$  when the system evolves unperturbed in the original  $\sigma$  attractor. We consider three fixed points of  $F_\sigma^{(3)}$  for stabilization. They correspond, respectively, to period-one, -three, and -six UPO's of the full system. For the period-one and -three UPO's, all modes  $A_j$  and  $B_j$  have the same period. For the period-six UPO, the  $A_j$  modes have period three, whereas the  $B_j$  modes have period six. Nonetheless, the sinus modes of this period-six UPO present the time symmetry  $B_j(n+3) = -B_j(n)$ . Analogously, three fixed points of  $F_\sigma^{(4)}$  are considered. These correspond, respectively, to period-one, -four, and -eight UPO's. The period-one UPO is the same as identified from  $F_\sigma^{(3)}$ . The time symmetries are now  $A_j(n+2) = A_j(n)$  and  $B_j(n+2) = -B_j(n)$  for period four, and  $A_j(n+4) = A_j(n)$  and  $B_j(n+4) = -B_j(n)$  for period eight. We recall that the maps  $F_\sigma^{(k)}$  are based on  $A_1$  and  $A_2$  alone. Inspection of  $A_j$  and  $B_j$  dynamics indicates that there is no period-two UPO of Eq. (2) with the parameter values considered.

Table I displays five stabilized orbits with different pe-

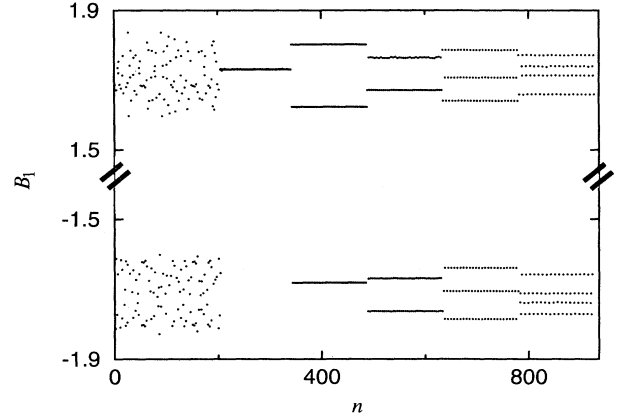


FIG. 2. Stabilization of five different UPO's in the KSE. Discrete time series of the Fourier coefficient  $B_1$  from Eq. (3), at the Poincaré section  $A_1=A_1^P=3.16$ ,  $A_1<0$ . Parameters are as in Fig. (1). From left to right: chaos and orbits of periods 1, 3, 4, 6, and 8. Notice the modified vertical scale.

riods. The maximum allowed  $|\delta\sigma|$  is different for each orbit. The largest  $|\delta\sigma|_{\max}$  is 0.3% of the nominal value of  $\sigma$ , and is used with the period-four UPO. The period-six and -eight UPO's are stabilized with the help of maps  $G^{(3)}$  and  $G^{(4)}$ , respectively. That is, in these two cases, control actions are performed twice per orbit, which allows for moderate values of  $|\delta\sigma|_{\max}$ . We concatenate in Fig. 2 the plots of  $B_1(n)$  corresponding to the UPO's listed in Table I. One sees, successively, chaotic behavior and stabilized orbits of period one, three, four, six, and eight. Figures 3 and 4 show, respectively, period-one and -three orbits, represented in the space of Eq. (2). Let us note that, for each of the orbits displayed in Figs. 3 and 4, another solution of Eq. (2) exists that is its mirror image around  $x = 0$ . On the other hand, the period-four, -six, and -eight UPO's listed in Table I are their own mirror image around  $x = 0$ .

We have shown that space-continuous extended systems displaying phase turbulence can be stabilized via a small adjustable feedback perturbation, into highly structured spatiotemporal regimes that are time periodic. In our approach the state of the system is monitored in

TABLE I. Quantities associated with the stabilization of the five orbits depicted in Fig. 2: discrete period of the UPO, order  $k$  of the maps  $F_\sigma^{(k)}$  and  $G^{(k)}$  used in the identification and stabilization of the UPO, period  $T$  of the orbit, fixed point  $A_2^*$  around which control is performed, gain  $g$  of the perturbation, and maximum allowed perturbation  $|\delta\sigma|_{\max}$ .

Period	Maps	$T$	$A_2^*$	$g$	$ \delta\sigma _{\max}$
1	3	4.70	-1.2035	-0.050	$6.0 \times 10^{-3}$
3	3	14.0	-1.1850	0.158	$1.9 \times 10^{-3}$
4	4	18.6	-1.1940	0.040	$7.5 \times 10^{-3}$
6	3	27.8	-1.1886	0.104	$2.9 \times 10^{-3}$
8	4	37.3	-1.1920	0.063	$4.7 \times 10^{-3}$

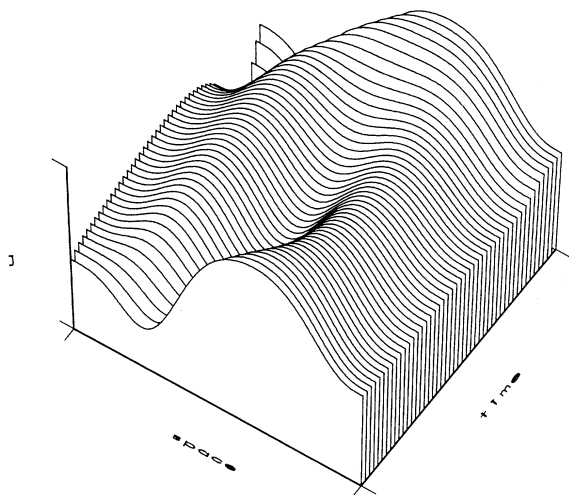


FIG. 3. Space-time diagram with one complete period-one orbit of the KSE. Scale is 13.0 for the  $u$  axis, 10.1 for space  $x$ , and 4.70 for time  $t$ . Time increases downwards.

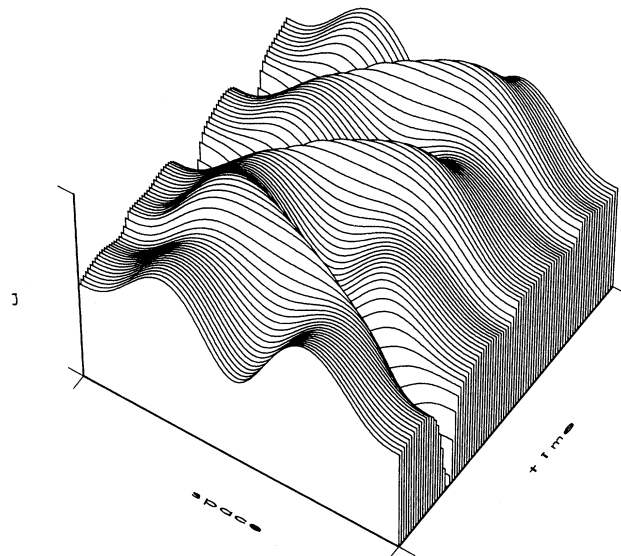


FIG. 4. Space-time diagram with one complete period-three orbit of the KSE. Scale is 13.1 for the  $u$  axis, 10.1 for space  $x$ , and 14.0 for time  $t$ . Time increases downwards.

Fourier space. Control of the flow associated with the time evolution of the Fourier coefficients induces a time periodic variation of the original system in physical space. It should be observed that the stabilization technique is more efficient whenever the system size is not large compared to the spatial correlation length. This is the case of the KSE with the parameter values considered, where a small number of modes with wavelengths comparable to the system size dominate. Difficulties of a technical nature arise in the control process as more modes contribute to the dynamics. Increasingly higher-dimensional control is required, and the use of a quasi-unidimensional map as part of the control algorithm may not suffice. Nonetheless, spatial normal modes appear to be the natural variables of the dynamics in “weakly nonlinear” regimes, instead of local quantities such as  $u(x_i)$  for a set  $\{x_i\}$ , each involving contributions from a number of those modes. The performance of the  $(m+1)$ -return map control relies to some extent on the ordering of characteristic times, and it is optimal if the convergence to the strange attractor is fast when compared to the exponential divergence from the embedded UPO. However, this is not a critical condition, inasmuch as the transient dynamics

between successive re-entries of the attractor is incorporated into the control map, and one does not simply wait passively for the transients to end. During those small transients, the system, in fact, performs moderate excursions from the controlled fixed point. These excursions are not harmful for control because they are rather limited in phase space and at the end of each  $(m+1)$  periods of recurrence the system is again in a close vicinity of the fixed point. No extraneous periodic orbits are introduced by the stabilization procedure. As noted in Ref. [3], the method of control can be applied even if the evolution equations of the system are not available. The method could be applied to experimental systems where a time series is monitored in a phase space spanned by Fourier coefficients, given that a parameter be accessible for small variations.

C.L. acknowledges the support of the Portuguese Government (JNICT-Programa CIENCIA, BD/1765/91-IA). M.H. was supported by the E.E.C. under the ESPRIT Contract No. P9282.

- [1] Y. Kuramoto, *Chemical Oscillations, Waves and Turbulence*, Springer Series in Synergetics (Springer-Verlag, Berlin, 1984).
- [2] A. Destexhe and A. Babloyantz, *Neural Comp.* **3**, 145 (1991).
- [3] E. Ott, C. Grebogi, and J. Yorke, *Phys. Rev. Lett.* **64**, 1196 (1990).
- [4] D. Ruelle, *Thermodynamic Formalism* (Addison-Wesley,

Reading, MA, 1978).

- [5] D. Auerbach, P. Cvitanović, J.-P. Eckmann, G. Gunaratne, and I. Procaccia, *Phys. Rev. Lett.* **58**, 2387 (1987).
- [6] F. Romeiras, E. Ott, C. Grebogi, and W. Dayawansa, in *Proceedings of the 1991 American Control Conference* (American Automatic Control Council, IEEE Service Center, Piscataway, NJ, 1991), pp. 1112–1119.

- [7] W. Ditto, S. Rauseo, and M. Spano, *Phys. Rev. Lett.* **65**, 3211 (1990).
- [8] V. Petrov, V. Gáspár, J. Masere, and K. Showalter, *Nature* **361**, 240 (1993).
- [9] A. Garfinkel, M. Spano, W. Ditto, and J. Weiss, *Science* **257**, 1230 (1992).
- [10] H. Gang and Q. Zhilin, *Phys. Rev. Lett.* **72**, 68 (1994).
- [11] J. A. Sepulchre and A. Babloyantz, *Phys. Rev. E* **48**, 945 (1993).
- [12] C. Lourenço and A. Babloyantz, *Neural Comp.* **6**, 1141 (1994).
- [13] A. Babloyantz and C. Lourenço, *Proc. Natl. Acad. Sci. U.S.A.* **91**, 9027 (1994).
- [14] I. Aranson, H. Levine, and L. Tsimring, *Phys. Rev. Lett.* **72**, 2561 (1994).
- [15] D. Auerbach, C. Grebogi, E. Ott, and J. Yorke, *Phys. Rev. Lett.* **69** 3479 (1992).
- [16] B. Nicolaenko, *Physica (Amsterdam)* **20D**, 109 (1986).
- [17] M. Jolly, I. Kevrekidis, and E. Titi, *Physica (Amsterdam)* **44D**, 38 (1990).